17th World Conference on Earthquake Engineering, 17WCEE
Sendai, Japan - September 13th to 18th 2020

Experimental study on moment resisting mechanism at pile and pile cap interface #2: Moment capacity formulation based on failure mechanism

Yusuke Tosauchi[1], Ryo Nakano[2], Shunsuke Naruse[3], Susumu Kono[4], Taku Obara[5]
Katsumi Kobayashi[6], Takeshi Fukuda[7], Yasuhiro Gunji[8] and Toshiaki Arai[9]

[1] *Researcher, Fujita Corporation, yusuke.tosauchi@fujita.co.jp*
[2] *Graduate student, Tokyo Institute of Technology, r3.rm.t2a@gmail.com*
[3] *Graduate student, Tokyo Institute of Technology, keromugi@icloud.com*
[4] *Professor, Tokyo Institute of Technology, kono.s.ae@m.titech.ac.jp*
[5] *Assistant Professor, Tokyo Institute of Technology, obara.t.ac@m.titech.ac.jp*
[6] *Managing Director, Fujita Corporation, katsumi.kobayashi@fujita.co.jp*
[7] *Researcher, Toda Corporation, takeshi.fukuda2@toda.co.jp*
[8] *Researcher, Nishimatsu Construction Co., yasuhiro_gunji@nishimatsu.co.jp*
[9] *Senior Researcher, Nishimatsu Construction Co., toshiaki_arai@nishimatsu.co.jp*

Abstract

In major earthquakes in Japan such as the 1995 Hyogo-ken Nanbu Earthquake, 2011 Tohoku Earthquake, and 2016 Kumamoto Earthquake, some buildings were demolished by losing their original functions because their piles and pile foundations were damaged leading to tilting of their superstructure. It is a new lesson for the Japanese engineering society that buildings can lose their functions even if the superstructure has no or very minor damage.

The bending behavior at the pile and pile cap interface was studied by Kirihara et al. in the 1980's. Their piles were embedded in pile caps as deep as their pile diameter. Several moment resisting mechanisms were clarified and modelled based on the experimental study and they proposed formulae for the bending capacity. However, recent piles have anchorage reinforcement to enhance the moment capacity with much smaller embedment length. In order to design for bending behavior at the interface, there are some issues to be quantified such as concrete strength enhancement due to the bearing effect of concrete, confining effect from reinforcement in the pile cap, volume of concrete in the pile cap which reacts against bending action, how rebar works in the pile cap.

This paper discusses the bending moment resisting mechanism and proposes moment capacity equations for the recent type of pile systems using the experimental work conducted on five specimens, which had short steel pile embedment (1/3*D* or 2/3*D* where *D* is the pile diameter) with or without anchorage reinforcement. Five specimens were designed to reach different types of concrete failure modes based on Kirihara et al.'s formulae. Test results showed unexpected failure modes and a new design equation is proposed. In the new equation, Kirihara et al.'s formulae were revised to take into account the effect of short embedment of pile, using Kokusho's study, and axial load ratio. The bending moment capacities based on the revised equation agreed well with the experimental results with good accuracy. Clarification of detailed resisting mechanism is still underway to cover a wider range of axial load ratio and amount of anchorage reinforcement, and to quantify deformation for different characteristic points in order to increase the accuracy of the equations and build performance based design criteria for the pile and pile cap interface.

Keywords: Pile and pile cap interface; Pile embedment length; Anchorage reinforcement; Moment resisting mechanism

1. Introduction

In recent years, efforts to understand the seismic behavior of pile foundations have increased and the need for secondary seismic design for piles in severe earthquake has become apparent. To address this, experimental investigations are conducted at different organizations in Japan [1,2]. The Architectural Institute of Japan (AIJ) is developing design guidelines based on the findings from these studies [3, 4].

Among different aspects of pile foundations, this series of studies are focused on the connection between pile and pile-cap. In particular, the moment resisting mechanism at the pile and pile cap interface is investigated. In the companion paper (Part 1), the authors presented experiments carried out on a pile cap with a short pile head embedding length, and reported the maximum strength and observed damage of the pile cap [5].

This part of the study (Part 2) focuses on developing expressions to predict the moment strength of the pile and pile cap interface based on the resistance mechanism for a laterally loaded pile. Related to this objective, Kirihara et al. [6] have provided equations for the moment strength for pile caps with long pile-head embedment length. They described different failure modes of the pile cap interface and methods for calculating the strength associated with each mode. The proposed solutions showed good agreement with the experimental results. However, the formulation proposed by Kirihara et al. [6] does not include the contribution from axial force in the pile. Furthermore, recently piles and pile caps are now often connected with a reinforcing bar welded to the pile head to shorten the length of pile-head embedment. The applicability of the expression proposed in [6] is still unclear for these cases of short pile-head embedment. Therefore, prior to the experiments described in Part 1 [5], the authors developed expressions to predict the moment strength of the pile and pile-cap interface including the effect of axial load on the pile. These expressions are based on the resistance mechanism of the pile and pile-cap interface when lateral load is applied to the pile.

The following sections present the different failure modes considered and corresponding moment-strength for each mode based on the resistance mechanisms. The accuracy of proposed expressions is validated by comparing the maximum strength and failure modes obtained from the experiments described in Part 1 [5].

Prior to the experiment, the authors modeled the resistance mechanism of the pile and pile cap interface when horizontal force was applied to the pile, and derived a calculation formula to predict the maximum strength of the pile cap interface. A calculation formula for pile caps with long pile head embedding length is proposed by Kirihara et al. [6]. The paper [6] describes some failure modes of pile cap interfaces and the method of calculating the maximum strength of each mode and it showed good correspondence with experimental results. But the method doesn't include the axial force. Also, piles and pile caps are new often fixed with a reinforcing bar welded to a pile head to shorten the length of the pile head embedment, but the applicability of Kirihara's formula in such a case is unclear.

Therefore, in Part 2, by comparing the predicted maximum strength with the maximum strength obtained in the experiment of Part 1 [5], the accuracy of the formula was confirmed taking into consideration the failure mode.

2. Failure modes

Kirihara et al. [6] present several failure modes for the pile-cap interface. Fig.1 shows typical failure modes. Failure mode 'b' is shear failure at the front of the pile cap interface, failure mode 'd' is tensile yielding perpendicular to the loading direction, failure mode 'e' is shear failure at the back of pile cap interface, and failure mode 'h' is slip failure at the back of pile cap interface. These failure modes are adopted herein for moment-strength calculation.

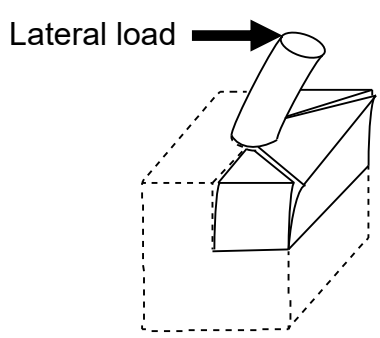

(a) Failure mode 'b' : Shear failure at front.

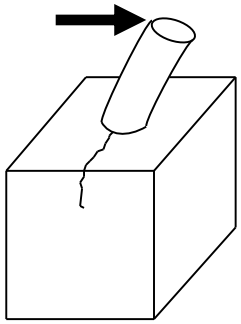

(b) Failure mode 'd' : Tensile yielding.

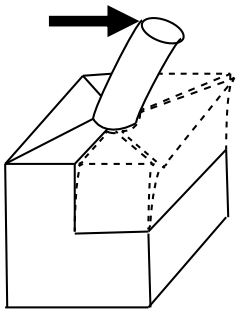

(c) Failure mode 'e' : Shear failure at back.

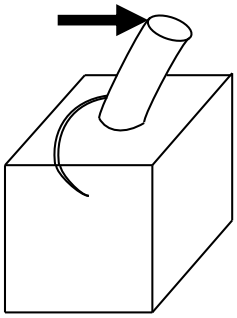

(d) Failure mode 'h' : Slip failure.

Fig.1— Failure modes of pile-cap for a laterally loaded pile [6].

As reported in Part 1 [5], the four specimens without rebar anchors developed cracks parallel to the loading direction on the front surface of the pile cap. Additionally, cracking was also observed in the direction perpendicular to loading, and these cracks extended toward the side of pile cap. Although the crack pattern is different from that in Fig. 1, the lateral load was reduced when the cracks perpendicular to the loading direction reached the side of the pile cap. Accordingly, the failure mode of these specimens was determined to be shear failure 'b'.

In the specimen having the pile-head rebar anchors, cracks formed in the front side the pile cap parallel to the loading direction and in the direction perpendicular to the loading toward the side of pile cap. Moreover, since cracks also occurred on the back surface of the load, the failure mode of the specimen was determined to be shear failure or bending failure in the front of the pile cap after bending failure at the back.

3. Modeling for resistance mechanisms

3.1 Formulation

First, referring to the stress distribution inside the pile cap interface reported by Kuromasa et al. [7], this study assumes the interaction force distributions as shown in Fig. 2 for long and short pile-head embedment. Model 1 (Fig. 2(a)) corresponds to the resisting mechanism for long pile-head embedment, and Model 2 (Fig. 2(b)) corresponds to the resisting mechanism for short pile-head embedment.

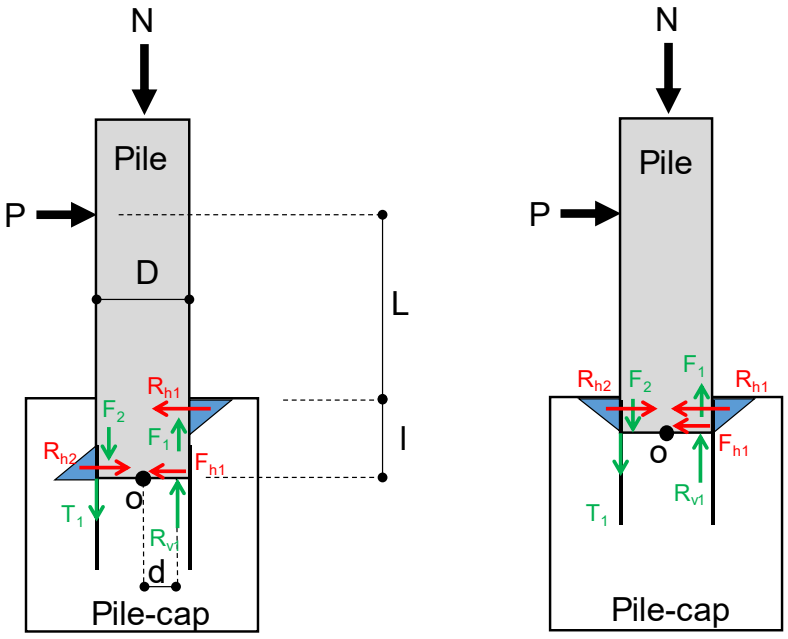

(a) Model 1 (b)Model 2

Fig.2 — Resistance mechanisms of pile pile-cap connection.

Referring to Fig. 2, the equilibrium of forces in horizontal and vertical direction yields the following for Model 1 and Model 2,

$$P + R_{h2} = R_{h1} + F_{h1} \tag{1}$$

$$F_1 + R_{v1} = N + F_2 + T_1 \tag{2}$$

where P is the applied horizontal load, R_{h1} and R_{h2} are the horizontal reaction forces acting on the pile from the pile cap, F_{h1} is the frictional force acting between the pile-head surface and the pile cap concrete, F_1 and F_2 are the frictional forces acting between the pile side and the pile cap, R_{v1} is the vertical reaction force acting on the pile from the pile-head joint surface, and N is the axial force.

Considering the equilibrium of moments about the point O, following equations can be obtained for Model 1 (Eq.(3)) and model 2(Eq.(4)),

$$P\ (L+l) + \frac{1}{6}lR_{h2} - \frac{5}{6}lR_{h1} - \frac{D}{2}F_1 - \frac{D}{2}F_2 - \frac{D}{2}T_1 - dR_{V1} = 0 \tag{3}$$

$$P\ (L+l) + \frac{2}{3}lR_{h2} - \frac{2}{3}lR_{h1} - \frac{D}{2}F_1 - \frac{D}{2}F_2 - \frac{D}{2}T_1 - dR_{V1} = 0 \tag{4}$$

where L is height of loading point from the pile cap surface, l is the embedment length, D is the pile diameter, T_1 is the tensile force at the pile head anchoring rebar, d is the vertical reaction force acting position and $d = (D/2) - (2t/3)$ (where t is the wall thickness of pile).

Equations (1)–(3) are used to determine P in Model 1; Eqs. (1), (2), and (4) are used to determine P in Model 2. The maximum lateral force P can be calculated given the horizontal reaction force R_{h1} in each failure mode.

Assuming that the coefficient of friction between the pile surface and the pile cap concrete is μ, the frictional forces F_1 and F_2 can be expressed as:

$$F_1 = \mu R_{h1}、\ F_2 = \mu R_{h2} \tag{5}$$

Substititing Eq.(5) into Eq.(2) gives,

$$R_{v1} = N + \mu R_{h1} + T_1 - \mu R_{h2} \tag{6}$$

Defining constants A and B as in Eq. (7), the expression for R_{h2} can be obtained as Eq. (8).

$$A = \frac{1}{6}l + \frac{1}{2}\mu D - \mu d、\quad B = \frac{1}{6}l - \frac{1}{2}\mu D - \mu d \tag{7}$$

$$R_{h2} = \frac{A}{B}R_{h1} + \frac{dN}{B} + \frac{DT_1}{2B} + \frac{dT_1}{B} - \frac{P(L+l)}{B} \tag{8}$$

As the coefficient of friction between the pile-head joint surface and the pile cap concrete is μ, F_{h1} can be expressed as,

$$F_{h1} = \mu R_{v1} = \mu(N + \mu R_{h2} - \mu R_{h1} + T_1) \tag{9}$$

Substituting Eqs. (8) and (9) into Eq. (1) gives the expression for P for Model 1 in terms of R_{h1} as,

$$P = \frac{(1-\mu^2)\left(1-\frac{A}{B}\right)R_{h1} - (1-\mu^2)\frac{dN}{B} - (1-\mu^2)\frac{DT_1}{2B} - (1-\mu^2)\frac{dT_1}{B} + \mu(N+T_1)}{1 - \frac{(1-\mu^2)(L+l)}{B}} \tag{10}$$

Following the similar procedure, the identical relationship between P and R_{h1} for Model 2 is obtained same as equation (10). However, for Model 2, constants A and B are defined as,

$$A = \frac{2}{3}l + \frac{1}{2}\mu D - \mu d、\quad B = \frac{2}{3}l - \frac{1}{2}\mu D - \mu d \tag{7}'$$

3.2 Capacity of each part

The maximum load P at failure mode is obtained as the summation of resisting capacities for different mechanisms. The following sections describe the calculation method for the capacity of each part. The expressions proposed in Kirihara et al. [6] are adopted herein and the details are omitted for brevity.

3.2.1 Shear strength at front and back

The shear strength of the front side and the back side of the pile cap is obtained using equation (11) as the summation of the shear strength of the concrete and shear strength of the reinforcing bar crossing the shear plane. Fig. 3 shows the area of the shear plane for the front and back sides.

$$Q_u = \frac{\sigma_B}{10} A_c + \frac{f_t}{\sqrt{3}} \frac{a_v}{2} \tag{11}$$

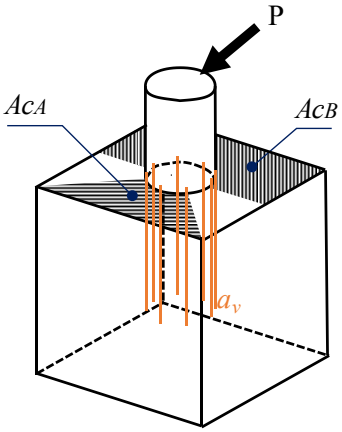

A_{CA} : Area of shear plane in front

A_{CB} : Area of shear plane in back

σ_B : Compressive strength of concrete

f_t : Tensile strength of reinforcement

a_v : Cross-sectional area of vertical reinforcement

Fig.3 — Area of shear planes.

3.2.2 Tensile strength

The tensile strength is the summation of the tensile strength of the reinforcement crossing the cracks shown in Fig. 4, and can be expressed as,

(12)

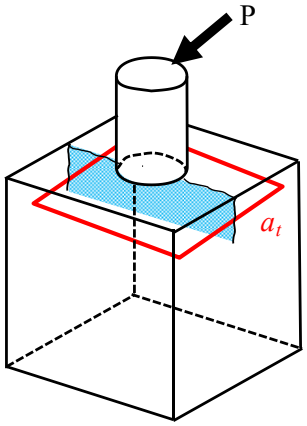

f_t : Tensile strength of reinforcement

a_t : Cross-sectional area of tensile reinforcement

Fig.4 — Schematic of reinforcement resisting the tensile failure.

3.2.3 Sliding failure strength

The slip failure strength of the back surface is calculated as Eq. (13). This value is taken as the summation of shear strength of concrete corresponding to the slip surface shown in Fig. 5, and the tensile strength and shear strength of the reinforcement crossing the cross section.

$$S_B = \frac{\sigma_B}{10} Bl + f_t a_t + \frac{f_t}{\sqrt{3}} \frac{a_v}{2} \tag{13}$$

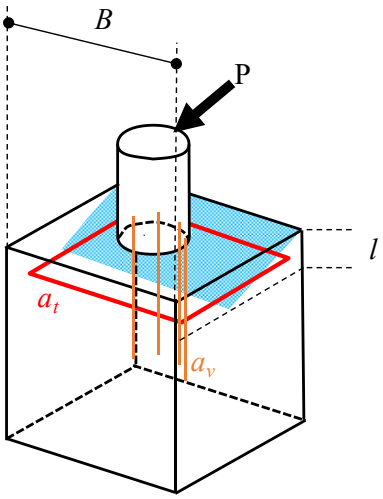

σ_B : Compressive strength of concrete

B : Width of pile cap

l : Embedment length of pile head

f_t : Tensile strength of reinforcement

a_t : Cross-sectional area of tensile reinforcement

a_v : Cross-sectional area of vertical reinforcement

Fig.5 — Area of concrete and reinforcement resisting slip failure.

3.2.4 Failure mode and reaction force R_{h1}

The horizontal reaction force R_{h1} acting on the pile from the pile cap according to each failure mode is calculated using Eq. (14) to (16). The failure modes 'bd' and 'be' are combination of two failure modes 'b'& 'd' and 'b'& 'e', respectively.

$$bd : R_{h1} = Q_{uA} + T_u \tag{14}$$

$$be : R_{h1} = Q_{uA} + Q_{uB} \tag{15}$$

$$h : R_{h1} = S_B \tag{16}$$

Finally, the maximum load P is calculated from Eq. (10) using Rh1 from Eqs. (14) to (16) for each failure mode.

4. Comparison of the experimental and calculated results

Table 1 shows the maximum strength corresponding to each failure mode obtained using the expressions described above. The strength of each specimen obtained from the experiment are also presented. The results are compared in terms of bending moment at the pile head joint surface. The bending moment M_{cal} is calculated using Eq. (17), and the experimental value M_{exp} is calculated using Eq. (18). In Eq. (18), δ is the horizontal displacement of the pile at the height where the axial force is introduced (Fig. 6).

$$M_{cal} = P \times (L + l) \tag{17}$$

$$M_{exp} = P \times (L + l) + N \times \delta \tag{18}$$

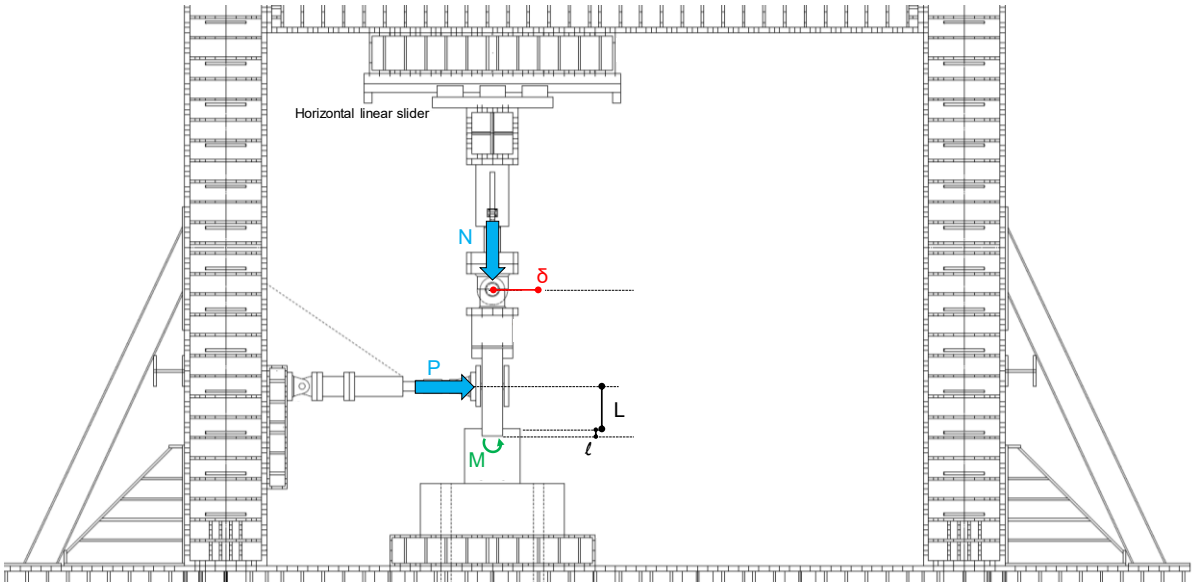

Fig.6 — Schematic of test setup.

Based on the calculation results, the specimens A01, A02, and A04 would be expected to fail in the failure mode ‘h’; however, the experimental results indicated the failure mode to be ‘bd’ or ‘be’. That is, the failure mode expected from the calculation results and the failure mode observed in the experiment were different. According to the experimental results, the strain of the concrete on the back side of the load was small. It is probable that the reaction force R_{h2} did not develop in the experiment because the embedding length of the pile head was short and the reinforcement around the pile head was smaller than that in the previous study [6].

Referring to the calculated maximum strength for these specimens (Table 1), the strength for failure mode ‘bd’ is relatively close to the experimental results. In addition, from the fact that the maximum strength of the failure mode ‘be’ is larger than that of failure mode ‘bd’, and based on the crack pattern observed in the experiment, the failure modes of the specimen A01, A02, and A04 are determined to be ‘bd’. Accordingly, Fig. 7 compares the experimental results to the calculation results for failure mode ‘bd’. For the specimens B01 and A19, the calculated values are close to the experimental results in Model 1. On the other hand, for test specimens A01, A02, and A04, the calculated values of the Model 2 are close to the experimental results.

Table 1 — Comparison of the experimental and calculated results

	Specimen	l	M_{cal} [kNm]			M_{exp}
			bd	be	h	[kNm]
Model 1	B01	0.67D	31.7	83.8	38.8	28.7
	A01	0.33D	23.6	59.4	17.4	20.0
	A02		30.0	61.1	23.6	23.1
	A04		47.2	78.6	40.7	36.7
	A19		39.4	69.6	46.0	40.7
	Specimen	l	M_{cal} [kNm]			M_{exp}
			bd	be	h	[kNm]
Model 2	B01	0.67D	18.9	47.1	22.7	28.7
	A01	0.33D	17.6	42.1	13.4	20.0
	A02		21.9	43.2	17.6	23.1
	A04		38.1	59.7	33.7	36.7
	A19		31.5	52.2	36.1	40.7

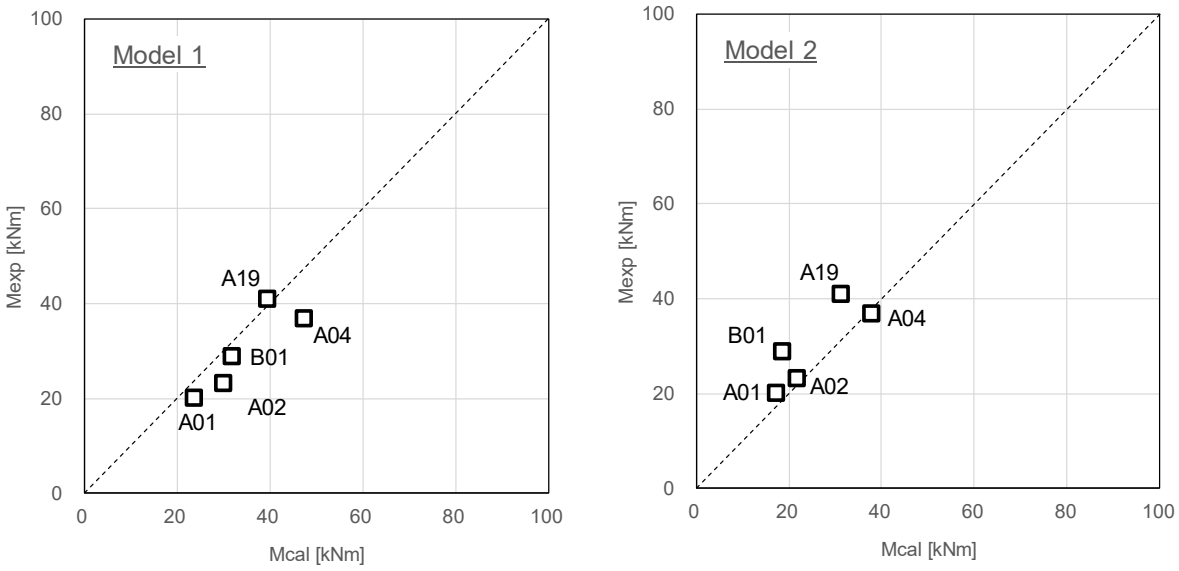

(a) Model 1 (b) Model

Fig.7 — Comparison of the experimental and calculated results for failure mode ‘bd’.

5. Conclusions

In this paper (Part 2 of a companion paper), expressions to calculate the moment-strength of the pile cap was derived, and the experimental results were compared with the calculated results. The findings from this study can be summarized as follows:

・The failure mode of all specimens is determined to be combination of shear failure at the front and tensile yielding (i.e., failure mode ‘bd’).

・For test specimens B01 and A19, the calculated values considering Model 1 are close to the experimental value, whereas for specimens A01, A02, and A04, the calculated values considering Model 2 are close to the experimental value.

However, the resistance mechanism assumed to predict the maximum strength and the resistance mechanism observed in the experiment were found to be different. In particular, slip failure ‘h’ was predicted

to control but did not. Therefore, future study will refine the modelling approach based on the resistance mechanism observed in the experiments, to develop reliable design formulae.

6. Acknowledgements

This work was supported by JSPS through two Grant-in-Aid programs (PI: Shuji Tamura, and Susumu Kono).

We are thankful to the Consortium for Socio-Functional Continuity Technology (PI: S. Yamada), the Collaborative Research Project (Materials and Structures Laboratory), and the World Research Hub Initiative (Institute of Innovative Research), at Tokyo Institute of Technology for their generous support of this research.

7. References

[1] Building Research Institute (2019) : Study on structural performance evaluation for concrete pile sub-assemble system with post-earthquake functional use. *Building Research Data*. No.195 [In Japanese]

[2] Mukai Tomohisa et al. (2017) : Study on structural performance evaluation for concrete pile system with post-earthquake functional use. *Summaries of technical papers of annual meet*ing, Architectural Institute of Japan, Hiroshima, Japan [in Japanese]

[3] Architectural Institute of Japan (2019) : Recommendations for design of building foundations [In Japanese]

[4] Architectural Institute of Japan (2017) : AIJ guidelines for seismic design of reinforced concrete foundation members [In Japanese]

[5] Naruse Shunsuke et al (2020) : Experimental study on moment resisting mechanism at pile and pile cap interface #1: Experimental Investigation. *17th World Conference on Earthquake Engineering*, Sendai, Japan

[6] Kirihara et al. (1986) : Failure and ductile capacity at steel-pile and pile-cap interface. *J. Struct. Constr. Eng., AIJ*.No.366, pp. 132-140, Japan [In Japanese]

[7] Kuromasa et al. (1981) : Study about pile and pile-cap interface during positive and negative lateral loading test. *Summaries of technical papers of annual meeting, Architectural Institute of Japan*, pp. 2327-2328, Japan [In Japanese]

